WHEN SPARSITY MEETS LOW-RANKNESS: TRANSFORM LEARNING WITH NON-LOCAL LOW-RANK CONSTRAINT FOR IMAGE RESTORATION

Bihan Wen, Yanjun Li and Yoram Bresler

Electrical and Computer Engineering and Coordinated Science Laboratory
University of Illinois at Urbana-Champaign, IL, USA.

ABSTRACT

Recent works on adaptive sparse signal modeling have demonstrated their usefulness in various image/video processing applications. As the popular synthesis dictionary learning methods involve NP-hard sparse coding and expensive learning steps, transform learning has recently received more interest for its cheap computation. However, exploiting local patch sparsity alone usually limits performance in various image processing tasks. In this work, we propose a joint adaptive patch sparse and group low-rank model, dubbed STROLLR, to better represent natural images. We develop an image restoration framework based on the proposed model, which involves a simple and efficient alternating algorithm. We demonstrate applications, including image denoising and inpainting. Results show promising performance even when compared to state-of-the-art methods.

Index Terms— Sparse representation, Image denoising, Image inpainting, Block matching, Machine Learning

1. INTRODUCTION

Sparsity of natural images with the synthesis [1, 2], or transform model [3, 4] has been widely used for image processing. As synthesis dictionary learning methods typically involve an NP-hard sparse coding step [5], approximate methods [6, 2] are widely used, which are not efficient for large-scale problems. Alternatively, the *transform model* provides cheap and exact sparse coding. It models a signal $u \in \mathbb{R}^n$ as approximately sparsifiable using a transform $W \in \mathbb{R}^{m \times n}$, i.e., $Wu = \alpha + e$, where $\alpha \in \mathbb{R}^m$ is sparse, and e is a small transform-domain modeling error. Natural images are well-known to be approximately sparse after analytical transforms, such as the discrete cosine transform (DCT). Recent work on sparsifying transform learning proposed efficient learning algorithms with convergence guarantees [3, 4], which turn out to be advantageous in applications including image / video processing [4, 7], magnetic resonance imaging (MRI) [8], and computational tomography (CT) [9].

Apart from the local structures exploited by the sparse priors, natural images contain non-local structures in the form of self-similarities, exploited by a long line of work starting with non-local means [10]. Various state-of-the-art image restoration methods – including BM3D [11], SSC [12], CSR [13], and GSR [14] – group similar patches within the image via block matching (BM), and impose non-local structural priors on these groups. Recent work on image restoration [15, 16], video denoising [17], compressed sensing image recovery [18], and cardiac cine MRI [19], introduced a low-rank prior to model similarity between patches within groups, and showed favorable results compared to other non-local image priors. More recently, local sparse priors and non-local low-rank priors have been simultaneously deployed for image restoration problems [20]. The low-rank prior was imposed on the data matrix formed by all patches, without grouping similar patches using BM.

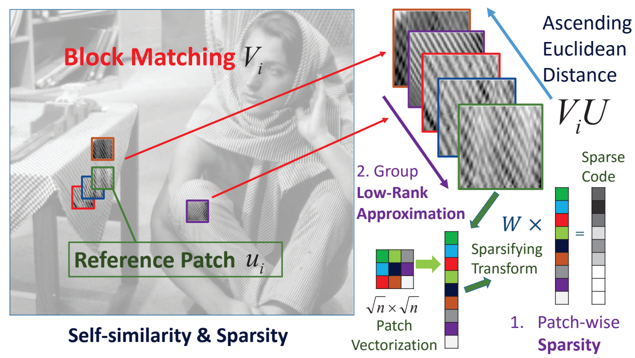

Fig. 1. A simple illustration of the STROLLR model for natural images, using group low-rankness and patch sparsity

In this paper, we propose a flexible Sparsifying TRansfOrm Learning and Low-Rank (**STROLLR**) model that combines the adaptive transform sparsity of image patches and the low-rankness of data matrices formed by BM, thus taking full advantage of both the local sparsity and non-local self-similarities in natural images. Figure 1 illustrates how STROLLR is used to model natural images. We develop variational image restoration formulations, for image denoising and inpainting, based on the proposed model. Efficient alternating algorithms are derived, with performance improvement over methods using local sparsity or low-rankness alone. We show promising numerical results over a set of testing images, even when compared to popular, or state-of-the-art methods.

2. STROLLR MODEL AND LEARNING

We propose the STROLLR model, in which the data matrix $U \in \mathbb{R}^{n \times N}$ is approximately sparsifiable by some transform $W \in \mathbb{R}^{m \times n}$, i.e., $WU = A + E$, where $A \in \mathbb{R}^{m \times N}$ is sparse, and E is the modeling error matrix with small Frobenius norm. Here $U = \left[u_1 \mid u_2 \mid ... \mid u_N \right]$, where each column $u_i \in \mathbb{R}^n$ denotes a signal. We define a BM operator $V_i : U \rightarrow V_i U \in \mathbb{R}^{n \times M}$, which takes u_i to be the reference patch, and selects M patches $\{u_j\}_i$ that are closest to u_i in terms of the Euclidean distance $\|u_j - u_i\|_2$. The selected patches $\{u_j\}_i$ form the columns of matrix $V_i U$ in ascending order of their Euclidean distance to u_i. (We order the patches so that V_i is well-defined, but the order *per se* has no effect on our model.) In addition to patch sparsity, the STROLLR model imposes a low-rank prior on each $V_i U$ via a matrix rank penalty. The joint sparse coding and low-rank approximation problem in STROLLR model is as follows,

$$(\text{P1}) \quad \left\{\hat{A}, \{\hat{D}_i\}\right\} = \underset{A,\{D_i\}}{\operatorname{argmin}} \; \|W\,U - A\|_F^2 + \gamma_s^2 \, \|A\|_0 + \gamma_l \sum_{i=1}^{N} \left\{ \|V_i\,U - D_i\|_F^2 + \theta^2 \, \text{rank}(D_i) \right\}$$

where the ℓ_0 "norm" counts the number of nonzeros in A, and $\text{rank}(\cdot)$ returns the rank of a matrix. To solve Problem (P1), one minimizes the modeling and approximation error, including both sparsity and rank penalties. The optimal $\hat{A}$ is called the sparse code matrix of U, and the optimal $\hat{D}_i$ is the low-rank approximation of the matched block $V_i\,U$. The low-rank prior has been widely used to model spatially similar patch groups [15, 17, 18, 19]. Figure 1 illustrates the relation between image self-similarity and the low-rank matrix $\{V_i\,U\}$ obtained from BM. Here, we use the penalty $\text{rank}(D_i)$ to impose a non-local structural prior, which leads to a simple low-rank approximation algorithm [16].

Instead of using analytical transforms, an adaptively learned W [4, 3] provides superior sparsity, which serves as a better regularizer [8, 7, 9]. Generally, the sparsifying transform W can be overcomplete [4] or square [3], with different types of regularizers or constraints [3]. In this work, we restrict ourselves to learning a square (i.e., $m = n$) and unitary (i.e., $W^T\,W = I_n$, where $I_n \in \mathbb{R}^{n \times n}$ is the identity matrix) transform [3], which leads to highly efficient learning and image restoration algorithms [21, 8]. Given the training data matrix U, the STROLLR learning problem is formulated as follows:

$$(\text{P2}) \quad \min_{\{W,A,\{D_i\}\}} \; \|W\,U - A\|_F^2 + \gamma_s^2 \, \|A\|_0 + \gamma_l \sum_{i=1}^{N} \left\{ \|V_i\,U - D_i\|_F^2 + \theta^2 \, \text{rank}(D_i) \right\} \;\; s.t. \;\; W^T W = I_n$$

Previous work proposed simple and exact solution for optimal unitary $\hat{W}$ [3] with fixed A. In Section 3, we introduce efficient and effective image restoration algorithms with the proposed STROLLR model.

3. IMAGE RESTORATION

3.1. Restoration Framework

We propose a patch-based image restoration framework based on STROLLR learning. The goal is to recover an image X by reconstructing all of its overlapping 2D patches $\{u_i\}_{i=1}^N$ ($u_i \in \mathbb{R}^n$) from their corrupted measurements $\{y_i\}$. The patch measurements are modeled as $y_i = B_i\,u_i + h_i$, where h_i is additive noise, and $B_i \in \mathbb{R}^{n \times n}$ is a corruption operator (e.g., $B_i = I_n$ in image denoising problem) for the i-th patch. We propose the following patch-based image restoration formulation using STROLLR learning,

$$(\text{P3}) \quad \min_{\{W,A,\{D_i,U\}\}} \; \|W\,U - A\|_F^2 + \gamma_s^2 \, \|A\|_0 + \gamma_l \sum_{i=1}^{N} \left\{ \|V_i\,U - D_i\|_F^2 + \theta^2 \, \text{rank}(D_i) \right\} + \gamma_f \sum_{i=1}^{N} \left\{ \|B_i\,R_i\,U - y_i\|_2^2 \right\} \;\; s.t. \;\; W^T W = I_n$$

where R_i selects the i-th column of U such that $R_i U = u_i$. The data fidelity term $\|B_i\,R_i\,U - y_p\|_2^2$ is imposed, with the weight γ_f. The BM operator V_i searches for the M most similar patches by computing and comparing the Euclidean distances between all patch pairs, which can be very expensive for restoring large X (i.e., N is large). In practice, we set a square $Q \times Q$ search window, which is centered at the reference patch [16]. Only the overlapping patches within the search window are evaluated by the BM operator, assuming the neighborhood patches normally have higher spatial similarities.

We propose a simple block coordinate descent algorithm framework to solve (P3). Each iteration involves four steps: (i) sparse coding, (ii) transform update, (iii) low-rank approximation, and (iv) image patch restoration. Once the iterations complete, we recover the image by performing an (v) aggregation step.

Sparse Coding. Given the training U and fixed W, we solve the Problem (P3) for the sparse codes,

$$\hat{A} = \underset{A}{\operatorname{argmin}} \; \|W\,U - A\|_F^2 + \gamma_s^2 \, \|A\|_0 \tag{1}$$

which is the standard transform-model sparse coding problem. The optimal $\hat{A}$ can be obtained using cheap hard thresholding, $\hat{A} = H_{\gamma_s}(W\,U)$. Here the hard thresholding operator $H_v(\cdot)$ is defined as

$$(H_v(Q))_{a,b} = \begin{cases} 0 & , \; |Q_{a,b}| < v \\ Q_{a,b} & , \; |Q_{a,b}| \geq v \end{cases}$$

where $Q \in \mathbb{R}^{n \times N}$ is the input matrix, v is the threshold, and the subscripts a, b index the matrix entries.

Transform Update. We solve for unitary W in (P3) with fixed A, which is equivalent to the following,

$$\hat{W} = \underset{W}{\operatorname{argmin}} \; \|W\,U - A\|_F^2 \quad s.t. \;\; W^T\,W = I_n \tag{2}$$

With the unitary constraint, the optimal $\hat{W}$ has a simple and exact solution. Denoting the full singular value decomposition (SVD) of $U\,A^T$ as $S\,\Sigma\,G^T$, the transform update is $\hat{W} = GS^T$.

Low-rank Approximation. With the BM operators $\{V_i\}$, we solve for each low-rank approximation D_i as,

$$\hat{D}_i = \underset{D_i}{\operatorname{argmin}} \; \|V_i\,U - D_i\|_F^2 + \theta^2 \, \text{rank}(D_i) \tag{3}$$

We form matrix $V_i\,U$ using BM within the search window, which is centered at u_i. Let $\Phi\Omega\Psi^T = V_i\,U$ be the full SVD, then $\hat{D}_i = \Phi H_\theta(\Omega)\Psi^T$ is the exact solution.

Patch Restoration. Each of the image patches is restored, with fixed A, W and $\{D_i\}$, by solving the following problem,

$$\hat{u}_i = \underset{u_i}{\operatorname{argmin}} \; \|W\,u_i - \alpha_i\|_2^2 + \gamma_f \, \|B_i\,u_i - y_i\|_2^2 + \gamma_l \sum_{j \in C_i} \|u_i - D_{j,i}\|_2^2 \tag{4}$$

where α_i denotes the i-th column of the sparse matrix A. The set C_i contains all indices j's such that the matrix $V_j U$ contains column u_i, i.e., $C_i = \{j : u_i \in V_j\,U\}$. Thus $D_{j,i} \in \mathbb{R}^n$ is the column of D_j, corresponding to the location of u_i in $V_j U$. The variations and solutions to this step in two exemplary applications will be discussed in Section 3.2.

Aggregation. Once the iterations complete, one can aggregate the restored patches to recover the image, by averaging pixels from weighted patches $\{\hat{u}_i\}$ at their respective locations in the image. Each patch $\hat{u}_i$ is weighted by the reciprocal of the sparsity of $\hat{\alpha}_i$, i.e., $1/\|\hat{\alpha}_i\|_0$, since a patch with higher sparsity usually contains more remaining corruption after restoration.

STROLLR Image Restoration Algorithm Framework

Input: The corrupted image Y, the initial transform W_0.
Initialize: $\hat{W}_0 = W_0$, $\hat{U}_0 = \left[R_1 Y \mid R_2 Y \mid ... \mid R_N Y\right]$.
For $t = 1, 2, ..., T$ **Repeat**

1. **Sparse Coding:** $\hat{A}_t = H_{\gamma_s}(\hat{W}_{t-1} \hat{U}_{t-1})$.
2. **Transform Update:** Compute $S_t \Sigma_t G_t^T = \mathrm{SVD}(\hat{U}_{t-1} \hat{A}_t^T)$ as the full SVD, then update $\hat{W}_t = \mathrm{SVD}(G_t S_t^T)$.
3. **Low-rank Approximation:**
   (a) Form $\{V_i\, U_{t-1}\}$ using BM.
   (b) Compute $\Phi_t \Omega_t \Psi_t^T = V_i\, U_{t-1}$.
   (c) Update $\hat{D}_{i,t} = \Phi_t H_\theta(\Omega_t) \Psi_t^T \; \forall i$.
4. **Patch Restoration:** Restore the patch with closed-form solution for denoising or inpainting, to update $\hat{U}_t$

End
Aggregate $\{\hat{u}_i\}_{i=1}^N$ to restore the image $\hat{X}$.

Fig. 2. STROLLR image restoration algorithm framework.

3.2. Image Denoising and Inpainting

In the patch restoration step, the solution to $\hat{u}_i$ depends on the operator B_i, which leads to different types of image restoration problems. We will discuss two examples, namely image inpainting, and denoising in this section. Both algorithms follow the same image restoration framework which is summarized in Fig. 2.

Robust Inpainting. When B_i is a diagonal binary matrix with zeros at the locations corresponding to missing pixels, (P3) becomes an image inpainting problem. The least squares solution to (P3) is $\hat{u}_i = \{(1 + |C_i|\gamma_l) I_n + \gamma_f B_i\}^{-1} (W^T \alpha_i + \gamma_l \sum_{j \in C_i} D_{j,i} + \gamma_f B_i y_i)$. Since both I_n and B_i are diagonal matrices, the matrix inverse and matrix-vector multiplication are simple and cheap.

Image Denoising. When $B_i = I_n$, we are solving the patch-based image denoising problem, with no pixel missing. The denoised patches are reconstructed as follow,

$$\hat{u}_i = \underset{u_i}{\mathrm{argmin}} \; \|W\, u_i - \alpha_i\|_2^2 + \gamma_f \|u_i - y_i\|_2^2 + \gamma_l \sum_{j \in C_i} \|u_i - D_{j,i}\|_2^2 \tag{5}$$

The optimal $\hat{u}_i$ has a simple least squares solution,

$$\hat{u}_i = (W^T \alpha_i + \gamma_f y_i + \gamma_l \sum_{j \in C_i} D_{j,i}) / (1 + \gamma_f + |C_i|\gamma_l) \tag{6}$$

where the denoised patch is equal to the weighted sum of its sparse code reconstruction, noisy measurement, and block-wise low-rank approximation.

4. EXPERIMENTS

We demonstrate the promise of the STROLLR based image restoration framework by testing our image inpainting and denoising algorithms on a set of 10 images, as shown in Fig. 3. We set γ_f to be inversely proportional to the noise standard deviation σ, i.e., $\gamma_f = \gamma_{f,0}/\sigma$, to reduce the penalty weight when the measurement becomes more noisy. Additionally, we set γ_l, γ_s, and θ to be proportional to σ, i.e., $\gamma_l = \sigma \gamma_{l,0}$, $\gamma_s = \sigma \gamma_{s,0}$ and $\theta = \sigma \theta_0$. In both

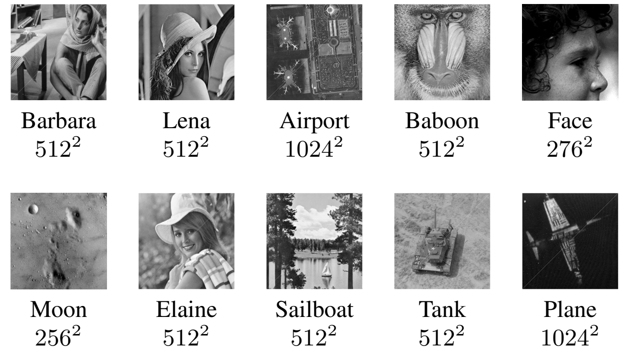

Fig. 3. Testing images used in the image denoising and image inpainting experiments, with names and sizes below.

Available pixels	σ	Smooth	LR	TL	STROLLR
20%	5	28.9	29.0	29.2	**29.3**
	10	27.4	28.2	28.2	**28.3**
	15	26.9	27.3	27.3	**27.4**
	20	25.5	**26.5**	26.2	**26.5**
10%	5	26.9	26.9	27.0	**27.1**
	10	26.0	26.3	26.3	**26.5**
	15	24.8	25.5	25.4	**25.6**
	20	23.7	24.7	24.5	**24.9**
Average		26.3	26.8	26.8	**27.0**

Table 1. PSNR values for image inpainting, averaged over 10 testing images, using patch smooth ordering (Smooth), TL based method, LR based method, and the STROLLR based method. The best PSNR value in each row is marked in bold.

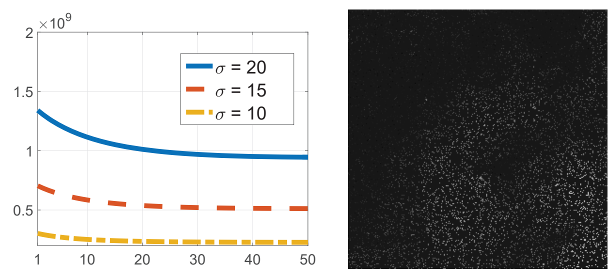

(a) STROLLR objective (b) Corrupted

(c) Inpainted (28.1dB) (d) Ground truth

Fig. 4. STROLLR inpainting illustration for image *Face*, with 90% pixels missing: (a) the plots of objective convergence, (b) the corrupted measurement, with noise $\sigma = 10$, (c) the inpainted result by STROLLR, and (d) the ground truth.

experiments, we set patch size $n = 64$, block size $M = 5n$, search window size $Q = 35$, the penalty weights $\theta_0 = 1.5$, and $\gamma_{s,0} = 2.5$. We initialize the sparsifying transform W_0 with the square 2D DCT. We remove the means of the extracted patches before the iterations, and add them back before the patch aggregation step. To evaluate the image restoration performance, we measure peak signal-to-noise ratio (PSNR) of the reconstructed images.

4.1. Image Inpainting

We present preliminary results for our STROLLR based inpainting method. We randomly remove 80%, and 90% of the pixels of the entire image, and simulate i.i.d. additive Gaussian noise for the sampled pixels with $\sigma = 5$, 10, 15, and 20. We set penalty weights $\gamma_{f,0} = 10$, and $\gamma_{l,0} = 1 \times 10^{-4}$. Figure 4(a) illustrates the convergence of the objective function over 50 iterations for inpainting image *Face* with only 10% pixels available, and noise $\sigma = 10$, 15, and 20. In practice, since the reconstruction PSNR saturates quickly, we set $T = 5$ for evaluating the image inpainting performance using STROLLR method, whose results are compared to those obtained by popular patch smoothing method [22]. Additionally, to show the effectiveness using both adaptive sparsity and low-rank regularizers for inpainting reconstruction, we also compare to the inpainting results that are obtained using only transform learning (TL) and group low-rank (LR) regularizers in reconstruction.

Table 1 lists the corrupted and inpainting PSNRs, averaged over all 10 testing images, obtained using the aforementioned methods, with the best result for each testing case marked in bold. Using both LR and TL regularizers, the proposed STROLLR based method performs well for all of the corruption cases. Figures 4(b), 4(c), and 4(d) visualize the the highly corrupted image *Face*, the inpainted result by the STROLLR based method, and the ground truth.

4.2. Image Denoising

We present image denoising results using our proposed algorithm in Sec. 3. We simulate i.i.d. Gaussian noise at 4 different noise levels ($\sigma = 5, 10, 15,$ and 20) for the testing images. We set $T = 1$, and penalty weights $\gamma_{f,0} = 1$, and $\gamma_{l,0} = 2 \times 10^{-3}$. Denoising results obtained using our proposed STROLLR based method are compared with those obtained by the adaptive K-SVD denoising scheme [2], the group low-rank approximation method (LR) [16], the square TL denoising scheme (TL) [3], and BM3D [11], which is a state-of-the-art image denoising method.

Table 2 lists the denoised PSNRs obtained using the aforementioned methods, with the best result for each testing case (i.e., each row) marked in bold. The proposed STROLLR image denoising method provides average PSNR improvements of 0.3dB, 0.2dB, 0.3dB, and 0.1dB, respectively, over the K-SVD, LR, TL, and BM3D denoising methods. Local sparsity based methods, such as K-SVD and TL, usually perform well for corrupted images with low noise σ, while non-local methods, such as LR and BM3D, denoise better when σ increases. By imposing both local (i.e., patch sparsity) and non-local (i.e., group low-rankness) regularizers, for all testing images and noise σ's, STROLLR performs consistently among the best. Thus our proposed method demonstrates robust and promising performance in image denoising compared to popular competing methods.

Images	σ	KSVD	LR	TL	BM3D	STROLLR
Barbara	5	38.1	38.4	38.1	38.3	**38.5**
	10	34.4	35.0	34.3	35.0	**35.1**
	15	32.3	33.1	32.1	33.1	**33.2**
	20	30.8	31.8	30.5	31.7	**31.9**
Lena	5	38.6	38.6	38.6	38.7	**38.8**
	10	35.5	35.8	35.5	**35.9**	**35.9**
	15	33.7	34.2	33.7	**34.3**	**34.3**
	20	32.4	33.0	32.2	33.0	**33.1**
Airport	5	35.7	35.6	35.8	35.8	**35.9**
	10	32.0	32.0	32.1	32.0	**32.2**
	15	30.2	30.3	30.2	30.2	**30.4**
	20	29.0	29.1	29.0	29.1	**29.2**
Baboon	5	35.2	35.1	35.2	**35.3**	**35.3**
	10	30.5	30.5	30.5	30.6	**30.7**
	15	28.0	28.2	28.1	28.2	**28.3**
	20	26.4	26.7	26.5	26.6	**26.8**
Face	5	**36.7**	36.5	36.6	**36.7**	**36.7**
	10	33.4	33.4	33.3	33.3	**33.5**
	15	31.9	**32.0**	31.8	**32.0**	**32.0**
	20	31.0	**31.3**	30.9	**31.3**	**31.3**
Moon	5	**36.1**	35.9	35.9	35.9	**36.1**
	10	**32.5**	32.3	**32.5**	32.1	**32.5**
	15	**30.9**	30.6	**30.9**	30.6	**30.9**
	20	**30.0**	29.6	29.9	29.8	**30.0**
Elaine	5	37.3	37.2	37.2	36.7	**37.4**
	10	34.0	34.1	33.7	33.3	**34.2**
	15	32.3	32.5	32.1	32.2	**32.6**
	20	31.4	31.6	31.2	31.5	**31.7**
Sailboat	5	36.7	36.5	36.6	36.6	**36.8**
	10	32.8	32.8	32.8	32.8	**33.0**
	15	31.0	31.0	30.9	**31.1**	**31.1**
	20	29.7	29.8	29.7	29.8	**29.9**
Tank	5	36.5	36.4	36.5	**36.6**	**36.6**
	10	33.1	**33.2**	33.0	33.1	**33.2**
	15	31.5	31.6	31.4	31.6	**31.7**
	20	30.4	30.5	30.3	30.6	**30.7**
Plane	5	**37.0**	**37.0**	36.7	36.7	**37.0**
	10	**34.3**	34.1	**34.3**	34.2	**34.3**
	15	33.2	33.3	33.3	33.3	**33.4**
	20	32.5	32.5	32.6	32.7	**32.8**
Average		32.9	33.0	32.8	33.1	**33.2**

Table 2. Comparison of image denoising PSNR values using K-SVD, group low-rank approximation method (LR), square TL denoising method (TL), BM3D, and the proposed STROLLR method. The average denoising PSNR values are calculated over all images and all noise levels for all methods. The best PSNR value in each row is marked in bold.

5. REFERENCES

[1] Michal Aharon, Michael Elad, and Alfred Bruckstein, "K-SVD: An algorithm for designing overcomplete dictionaries for sparse representation," *IEEE Trans. on Signal Processing*, vol. 54, no. 11, pp. 4311–4322, 2006.

[2] M. Elad and M. Aharon, "Image denoising via sparse and redundant representations over learned dictionaries," *IEEE Trans. Image Process.*, vol. 15, no. 12, pp. 3736–3745, 2006.

[3] S. Ravishankar and Y. Bresler, "ℓ_0 sparsifying transform learning with efficient optimal updates and convergence guarantees," *IEEE Transactions on Signal Processing*, vol. 63, no. 9, pp. 2389–2404, 2014.

[4] B. Wen, S. Ravishankar, and Y. Bresler, "Structured overcomplete sparsifying transform learning with convergence guarantees and applications," *Int. J. Computer Vision*, vol. 114, no. 2, pp. 137–167, 2015.

[5] G. Davis, S. Mallat, and M. Avellaneda, "Adaptive greedy approximations," *Journal of Constructive Approximation*, vol. 13, no. 1, pp. 57–98, 1997.

[6] Y. Pati, R. Rezaiifar, and P. Krishnaprasad, "Orthogonal matching pursuit : recursive function approximation with applications to wavelet decomposition," in *Asilomar Conf. on Signals, Systems and Comput.*, 1993, pp. 40–44 vol.1.

[7] B. Wen, S. Ravishankar, and Y. Bresler, "Video denoising by online 3d sparsifying transform learning," in *IEEE International Conference on Image Processing (ICIP)*, 2015, pp. 118–122.

[8] S. Ravishankar and Y. Bresler, "Data-driven learning of a union of sparsifying transforms model for blind compressed sensing," *IEEE Transactions on Computational Imaging*, vol. 2, no. 3, pp. 294 – 309, 2015.

[9] L. Pfister and Y. Bresler, "Tomographic reconstruction with adaptive sparsifying transforms," in *IEEE International Conference on Acoustics, Speech and Signal Processing (ICASSP)*, 2014, pp. 6914–6918.

[10] A. Buades, B. Coll, and J. M. Morel, "A non-local algorithm for image denoising," in *IEEE Comput. Soc. Conf. Comput. Vision and Pattern Recognition (CVPR 2005)*, June 2005, vol. 2, pp. 60–65 vol. 2.

[11] K. Dabov, A. Foi, V. Katkovnik, and K. Egiazarian, "Image denoising by sparse 3-d transform-domain collaborative filtering," *IEEE Trans. Image Process.*, vol. 16, no. 8, pp. 2080–2095, Aug 2007.

[12] J. Mairal, F. Bach, J. Ponce, G. Sapiro, and A. Zisserman, "Non-local sparse models for image restoration," in *IEEE 12th Int. Conf. Comput. Vision (ICCV 2009)*, Sept 2009, pp. 2272–2279.

[13] W. Dong, X. Li, L. Zhang, and G. Shi, "Sparsity-based image denoising via dictionary learning and structural clustering," in *IEEE Conf. Comput. Vision and Pattern Recognition (CVPR 2011)*, June 2011, pp. 457–464.

[14] J. Zhang, D. Zhao, and W. Gao, "Group-based sparse representation for image restoration," *IEEE Trans. Image Process.*, vol. 23, no. 8, pp. 3336–3351, Aug 2014.

[15] W. Dong, G. Shi, and X. Li, "Nonlocal image restoration with bilateral variance estimation: A low-rank approach," *IEEE Trans. Image Process.*, vol. 22, no. 2, pp. 700–711, Feb 2013.

[16] Haijuan Hu, Jacques Froment, and Quansheng Liu, "Patch-based low-rank minimization for image denoising," *arXiv preprint arXiv:1506.08353*, 2015.

[17] H. Ji, C. Liu, Z. Shen, and Y. Xu, "Robust video denoising using low rank matrix completion," in *IEEE Conf. Comput. Vision and Pattern Recognition (CVPR 2010)*, June 2010, pp. 1791–1798.

[18] W. Dong, G. Shi, X. Li, Y. Ma, and F. Huang, "Compressive sensing via nonlocal low-rank regularization," *IEEE Trans. Image Process.*, vol. 23, no. 8, pp. 3618–3632, Aug 2014.

[19] H. Yoon, K. S. Kim, D. Kim, Y. Bresler, and J. C. Ye, "Motion adaptive patch-based low-rank approach for compressed sensing cardiac cine mri," *IEEE Trans. Med. Imag.*, vol. 33, no. 11, pp. 2069–2085, Nov 2014.

[20] J. Li, X. Chen, D. Zou, B. Gao, and W. Teng, "Conformal and low-rank sparse representation for image restoration," in *IEEE Int. Conf. Comput. Vision (ICCV 2015)*, Dec 2015, pp. 235–243.

[21] B. Wen, S. Ravishankar, and Y. Bresler, "Learning flipping and rotation invariant sparsifying transforms," in *IEEE International Conference on Image Processing (ICIP)*, 2016, pp. 3857–3861.

[22] Idan Ram, Michael Elad, and Israel Cohen, "Image processing using smooth ordering of its patches," *IEEE transactions on image processing*, vol. 22, no. 7, pp. 2764–2774, 2013.